International Journal of Pharmaceutics 420 (2011) 84–92

Contents lists available at SciVerse ScienceDirect

International Journal of Pharmaceutics

journal homepage: www.elsevier.com/locate/ijpharm

Evaluation of the physical and biological properties of hyaluronan and hyaluronan fragments

Elaine L. Ferguson[a,b,*], Jessica L. Roberts[a,b], Ryan Moseley[a,b], Peter C. Griffiths[b,c], David W. Thomas[a,b]

[a] Wound Biology Group, Tissue Engineering and Reparative Dentistry, School of Dentistry, Cardiff University, Heath Park, Cardiff, CF14 4XY, UK
[b] Cardiff Institute of Tissue Engineering and Repair (CITER), Cardiff University, Cardiff, CF14 4XY, UK
[c] School of Chemistry, Cardiff University, Main Building, Park Place, CF10 3AT, UK

ARTICLE INFO

Article history:
Received 15 June 2011
Received in revised form 10 August 2011
Accepted 15 August 2011
Available online 22 August 2011

Keywords:
Hyaluronan
Wound healing
Polymer therapeutics
Hyaluronidase

ABSTRACT

Hyaluronan (HA) has been extensively used for various medical applications, including osteoarthritis, tissue augmentation and ocular surgery. More recently, it has been investigated for use in polymer therapeutics as a carrier for drugs and biologically active proteins, thanks to its biodegradability, biocompatibility and inherent biological properties. Such biological functions are strongly dependent on HA's chain length, yet the molecular weight of HAs used in polymer conjugates varies widely and is inconsistent with its intended application. Therefore, this study aimed to determine the ideal chain length of HA to be used in polymer conjugates for enhanced tissue repair.

HA fragments (M_w 45,000–900,000 g/mol) were prepared by acid hydrolysis of rooster comb HA and their physicochemical and biological properties were characterized. Such HA fragments had a highly extended, almost rod-like solution conformation and demonstrated chain length- and concentration-dependent viscosity, while exposure to HAase caused a rapid reduction in HA viscosity, which was most significant for the native HA. Initial HA hydrolysis rate by HAase varied strongly with HA chain length and was dependent on the formation of a stable enzyme–substrate complex. When normal human dermal fibroblasts were exposed to the different HA fragments for 72 h, only native (900,000 g/mol) HA reduced proliferation at 1000 μg/mL. Conversely, only the smallest HA fragment (70,000 g/mol) reduced the proliferation of chronic wound fibroblasts, at 1000 μg/mL. The 70,000 g/mol HA fragment also promoted the greatest cell attachment.

These observations demonstrate that low molecular weight (70,000–120,000 g/mol) HA fragments would be best suited for the delivery of proteins and peptides with applications in chronic wound healing and paves the way for the rationalized development of novel HA conjugates.

1. Introduction

Although considerable progress has been made in the field of regenerative medicine, many chronic conditions still prove difficult to treat effectively, due to the complex mechanisms of repair (Herrick et al., 1992). The use of water-soluble polymers in 'polymer therapeutics' was first described by Duncan (2003), and have been extensively investigated as anticancer nanomedicines. More recently, polymer conjugates, using the biologically inert dextrin, have been developed to promote tissue repair (Hardwicke et al., 2008, 2010, 2011). We have also demonstrated that hyaluronan (HA), a biologically active biopolymer, can be conjugated to trypsin and epidermal growth factor (EGF) to increase resistance to proteolytic degradation (Ferguson et al., 2010). To date, however, the molecular weight of HA used in polymer conjugates has varied widely and is inconsistent with the intended therapeutic indication (summarized in Table 1). Therefore, this study sought to determine the optimum molecular weight of HA for use as a component of polymer–protein conjugates for tissue repair purposes.

HA is a naturally occurring linear polysaccharide that is biodegradable, biocompatible and non-toxic. It is a macromolecule of several million Daltons, consisting of repeating units of D-N-acetylglucosamine and D-glucuronic acid (Linker and Mayer, 1954) that has been widely investigated for its tissue reparative effects, due to its multiple potential functions in normal wound healing responses. While some polymers are biologically inert, HA has a crucial role in tissue repair (Itano, 2008). HA displays antioxidant properties, and can modulate wound healing by promoting cell migration and proliferation, facilitating white blood cell infiltration and improving tissue hydration (Chen and Abatangelo, 1999; Price et al., 2007). However, these effects depend, in part, on the molecular size of HA (Huang et al., 2009; Stern

* Corresponding author at: Wound Biology Group, Tissue Engineering and Reparative Dentistry, School of Dentistry, Cardiff University, Heath Park, Cardiff, CF14 4XY, UK. Tel.: +44 0 2920 745454; fax: +44 0 29 20742442.
E-mail address: FergusonEL@cf.ac.uk (E.L. Ferguson).

0378-5173/$ – see front matter © 2011 Elsevier B.V. All rights reserved.
doi:10.1016/j.ijpharm.2011.08.031

Table 1
Examples of HA conjugates under development for clinical uses.

Therapeutic agent	Indication	HA molecular weight (g/mol)	Reference
Methotrexate	Osteoarthritis	2,000,000	Homma et al. (2009)
Cisplatin	Breast cancer	35,000	Cai et al. (2008)
Dexamethasone	Inflammatory diseases	490,000 1,360,000	Ito et al. (2007)
Bisphosphonate	Cancer	2,000,000	Varghese et al. (2009)
Quantum dots	Lymphatic vessel imaging	3000	Bhang et al. (2009)
Ribonuclease A	Cancer	130,000	Gilbert (2007)
CWRYMVm (peptide for FPRL1 receptor)	Inflammatory diseases	200,000	Oh et al. (2008)

and Maibach, 2008). It has been suggested that low molecular weight HA (1300–6800 g/mol) stimulates endothelial cell proliferation and immunological responses, whereas native HA can inhibit the formation of new blood vessels (Cui et al., 2009; West and Kumar, 1989). Although HA is used in its native high molecular weight, polydisperse form for various medical applications, such as osteoarthritis, ocular surgery, tissue augmentation and cutaneous wound healing (Chen and Abatangelo, 1999; Price et al., 2007; Wang et al., 2004), there is growing interest in using HA and its derivatives for the delivery of therapeutic proteins, peptides and nucleotides (Oh et al., 2010). While some research has focused on using HA derivatives for drug delivery, such derivatization can alter its biodegradation, toxicity and biological activity (Schanté et al., 2011), which could have vast preclinical safety and regulatory implications (Gaspar and Duncan, 2009). Duncan et al. recently described the Polymer masked-UnMasked Protein Therapy (PUMPT) concept, which uses biodegradable polymers, such as dextrin and HA, to mask and restore the biological activity of peptides and proteins (Duncan et al., 2008; Gilbert and Duncan, 2006). Ideally, polymers for PUMPT should be sufficiently large enough to 'mask' the therapeutic protein, but must be capable of penetrating tissues and be effectively removed from the body without causing toxicity or immune reactions.

Here, HA fragments of different chain lengths were prepared by acid hydrolysis and characterized using gel permeation chromatography (GPC), pulsed-gradient spin-echo NMR (PGSE-NMR), Fourier transform infrared spectroscopy (FTIR) and rheometry to assess solution properties and biodegradation of the HA fragments. Hyaluronidase (HAase) activity towards the HA fragments was also assessed. The effect of HA molecular weight and concentration on cell proliferation and adhesion was subsequently studied.

2. Materials and methods

2.1. Materials and cells

Hyaluronan from rooster comb, hyaluronidase (Type I-S) from bovine testes, bovine serum albumin (BSA), tissue culture grade dimethyl sulfoxide (DMSO), crystal violet, 3-(4,5-dimethylthiazol-2-yl)-2,5-diphenyltetrazolium bromide (MTT), trypan blue and optical grade DMSO were all from Sigma–Aldrich (Poole, UK). Sodium acid phosphate, sodium phosphate, sodium chloride, potassium phosphate, sodium acetate and hydrochloric acid (HCl) were purchased from Fisher Scientific (Loughborough, UK). Pullulan gel filtration standards (M_w = 11,800–788,000 g/mol) were from Polymer Laboratories (Church Stretton, UK). Unless otherwise stated, all chemicals were of analytical grade. All solvents were of general reagent grade (unless stated) and were from Fisher Scientific (Loughborough, UK).

Chronic wound and normal dermal fibroblasts were derived from biopsies of the edge of a chronic venous leg ulcer and from the ipsilateral thigh of the same patient, respectively (Wall et al., 2008), and subsequently hTERT (human telomerase, reverse transcriptase) immortalized. Cells were screened before use and found to be free of mycoplasma contamination. Dulbecco's minimum essential media (DMEM), fetal calf serum (FCS) and 0.05%, w/v trypsin-0.53 mM EDTA were obtained from Invitrogen Life Technologies (Paisley, UK).

2.2. Acid hydrolysis of HA

When the effects of temperature and incubation time on HA acid hydrolysis were being investigated, HA ($M_w \sim 900{,}000$ g/mol) was first dissolved in pre-warmed HCl (3 mg/mL, 0.4 M at 25, 40 or 60 °C) in a 100 mL round-bottomed flask under stirring, for up to 16 h. At various time intervals, samples (5 mL) were withdrawn from the flask. This mixture was immediately cooled and neutralized using an equimolar quantity of NaOH (1 M), before freezing and lyophilization.

When HA acid hydrolysis was scaled up for analysis, HA ($M_w \sim 900{,}000$ g/mol) was dissolved in pre-warmed HCl (3 mg/mL, 0.4 M at 40 or 60 °C) in a 100 mL round-bottomed flask under stirring, for up to 16 h. At 30 min intervals, samples (100 μL) were withdrawn from the flask and assessed for M_w using GPC (TSK G5000PW$_{XL}$ and G4000PW$_{XL}$ columns (Polymer Laboratories, Church Stretton, UK) in series, mobile phase phosphate buffered saline (PBS) (0.1 M, pH 7.4), flow rate of 1 mL/min), to measure its approximate molecular weight and polydispersity (compared to pullulan standards). The eluate was monitored using a differential refractometer (Gilson 153). Cirrus GPC software, version 3.2, from Polymer Laboratories (Church Stretton, UK) was used for data analysis. When the desired molecular weight was attained, the reaction mixture was immediately cooled and neutralized using an equimolar quantity of NaOH (1 M) before transferring the solution into dialysis membrane (molecular weight cut-off 2000 g/mol) and dialyzing against 4 × 5 L double distilled water (ddH_2O). The solution was lyophilized to yield degraded HA product as a white solid (~60% yield) that was characterized by FTIR (Avatar 360 ESP spectrophotometer with EZ OMNIC ESP 5.2 software; Thermo Nicolet, Loughborough, UK) and ^{1}H NMR to confirm identity, and by GPC (as above).

2.3. Pulsed-gradient spin-echo NMR (PGSE-NMR)

Pulsed-gradient spin-echo NMR experiments were carried out on a Bruker AMX360 NMR spectrometer, operating at 360 MHz (^{1}H) and using a stimulated echo-sequence, as described elsewhere (Davies and Griffiths, 2003). For each measurement, a 5 mm diffusion probe and a Bruker gradient spectroscopy accessory unit was used. All experiments were conducted at 37 °C. Temperature stability was maintained by the standard air heating/cooling system of the spectrometer, to an accuracy of ±0.3 °C.

The self-diffusion coefficients were extracted by fitting the peak amplitudes according to Eq. (1):

$$A(\delta, G, \Delta) = A_o \exp[(-kD_s)] \quad (1)$$

A is the peak amplitude in the absence (A_o) or presence $A(\delta, G, \Delta)$ of the field gradient pulses of duration δ (400 μs < δ < 2.8 ms), ramp time σ (250 μs), intensity G (0.86 T m^{-1}) and separation Δ (140 ms)

Table 2
Characteristics of HA fragments.

Fraction name	Degradation conditions	M_w (g/mol)[a]	M_n (g/mol)[a]	M_w/M_n
HA1	Native	895,000	513,000	1.74
HA2	40 °C, 7 h	360,000	233,000	1.54
HA3	60 °C, 4 h	119,500	47,500	2.51
HA4	60 °C, 16 h	67,500	24,500	2.76
HA5	60 °C, 18 h	42,500	16,000	2.66

[a] Estimated using GPC and pullulan standards (see text for details).

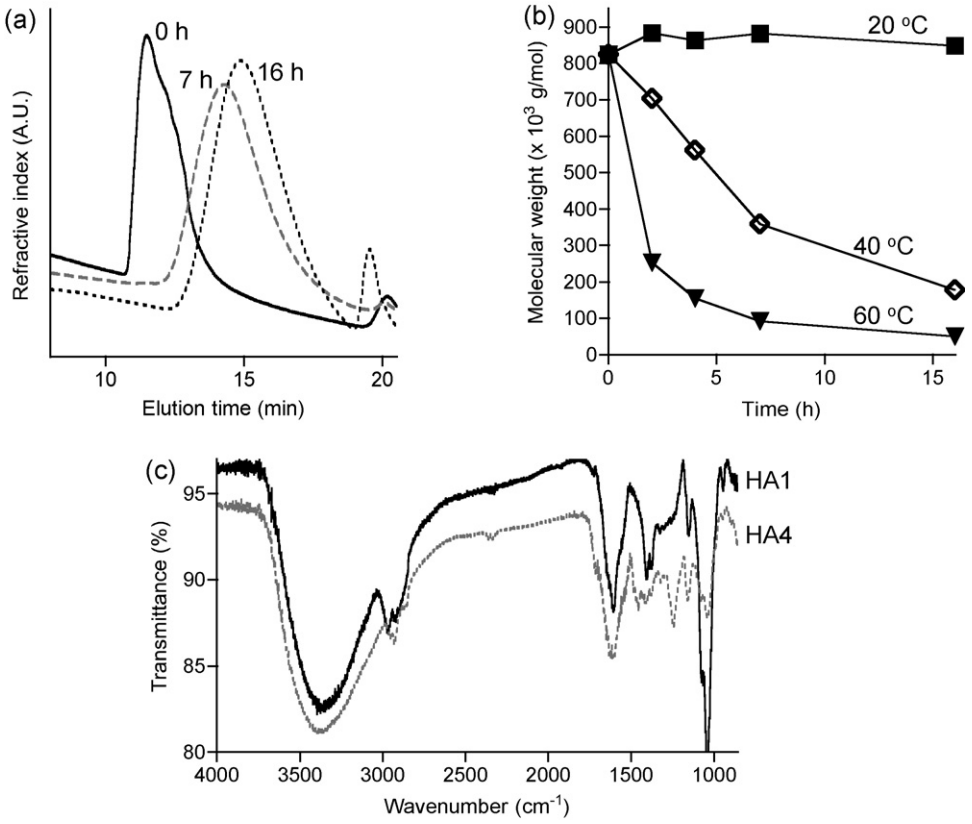

Fig. 1. Degradation of HA by acid hydrolysis. Panel (a) shows a typical GPC elution profile of HA, dissolved in 0.4 M HCl at 60 °C for 0 h (—), 7 h (- - -) and 16 h (. . .). Panel (b) shows the time-dependent change in relative molecular weight (GPC analysis) for HA dissolved in HCl (0.4 M) at 20, 40 and 60 °C. Panel (c) shows the FTIR profiles of HA1 and HA4.

where k is given by Eq. (2):

$$k = -\gamma^2 G^2 \left(\frac{30\Delta\left(\delta+\sigma\right)^2 - \left(10\delta^3 + 30\sigma\delta^2 + 35\sigma^2\delta + 14\delta^3\right)}{30} \right) \quad (2)$$

where γ is the gyromagnetic ratio.

2.4. Effect of molecular weight on HA viscosity

Viscosity was measured using a stress-controlled Bohlin CS10 rheometer (Bohlin Rheology, Lund, Sweden) with a parallel plate system (diameter, 20 mm; gap, 150 μm). The rheometer was controlled using Bohlin Rotational software, version 6.40.5.33. Temperature was maintained at 37 °C within the environmental chamber. HA fragments were dissolved in PBS (2–10 mg/mL) and applied to the rheometer test plate. Stress was applied for 20 s to increase the shear rate logarithmically from 0.06 to 430 s^{-1}, for up to a 7 min incubation.

When the effect of HAase-mediated degradation on HA viscosity was measured, pre-warmed (37 °C) HA solutions (250 μL) were gently mixed with PBS containing HAase (250 μL) to reach final concentrations of 2 mg/mL and 0–10 U/mL, respectively. The measurements usually started 60 s after mixing. The viscosity of the samples was measured as described above, after a 10 min incubation at 37 °C.

2.5. Hyaluronidase activity towards HA fractions

HAase activity was measured using a turbidimetric assay (adapted from (Dorfman and Ott, 1948)). Briefly, HA solutions (50 μL, 160 μg/mL in PBS, pH 5.3) were added to the wells of a 96-well plate and allowed to equilibrate at 37 °C for 30 min. HAase solution (50 μL, 4 U/mL in PBS, pH 6.9, containing 1 mg/mL BSA) was added to each well of the first column and the plate was incubated at 37 °C. At 10 min intervals, the HAse solution was added to the next column. After 30 min, a sample from each well (25 μL) was immediately transferred to a fresh plate containing acid albumin solution (125 μL, pH 3.8) and incubated for a further 10 min at 37 °C. Absorbance was read at 600 nm. Control wells contained no HA or HAase. HAase activity was expressed as change in absorbance per min.

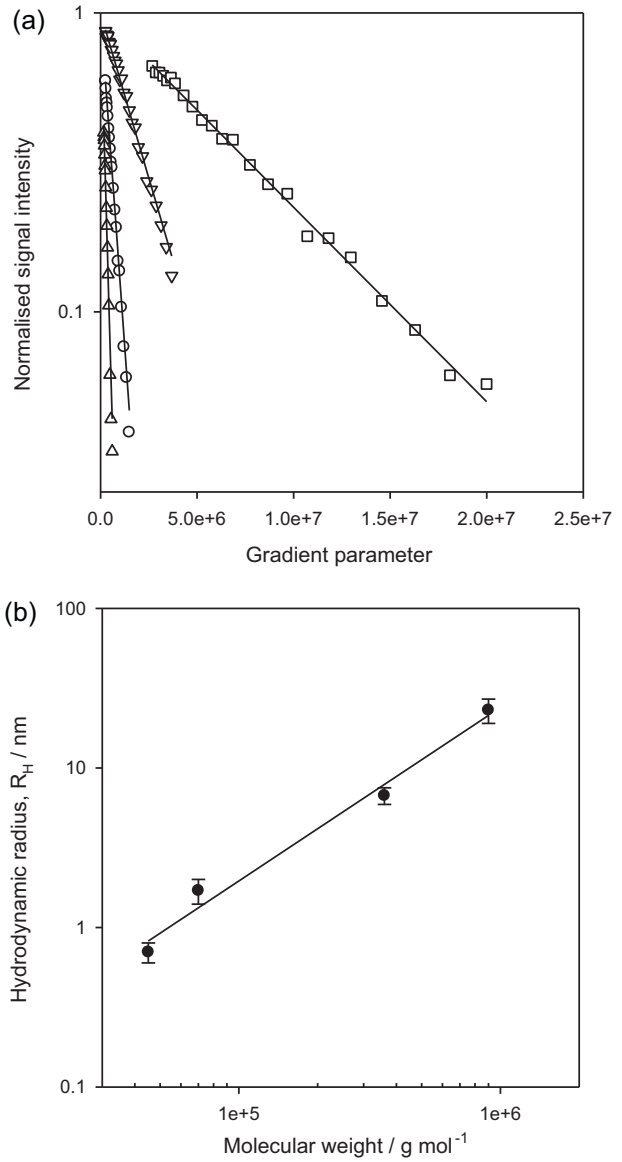

Fig. 2. Typical PGSE-NMR dataset for HA fragments. Panel (a) shows typical attenuation of HA solutions (10 mg/mL in D_2O, 37 °C), where □ = HA1 (900,000 g/mol); ○ = HA2 (360,000 g/mol); △ = HA4 (70,000 g/mol) and ▽ = HA5 (45,000 g/mol). Panel (b) shows the hydrodynamic radii of HA fragments, calculated from the self-diffusion coefficients via the Stokes–Einstein equation, as a function of molecular weight.

2.6. Fibroblast proliferation upon incubation with HA fractions

The MTT assay (Mosmann, 1983) was used to assess cell proliferation (72 h incubation at 37 °C/5% CO_2) in chronic wound and normal dermal fibroblasts. Cells were seeded into sterile 96-well microtitre plates (2.5×10^4 cells/mL) in 0.1 mL/well of DMEM media containing heat-inactivated FCS (10%, v/v) and allowed to adhere for 24 h. The culture medium was removed and the HA fragments, dissolved in fresh medium (0.2 μm filter-sterilized), were added. After a further 67 h incubation, MTT (20 μL of a 5 mg/mL solution in PBS) was added to each well and the cells incubated for a further 5 h. The medium was then removed and the precipitated formazan crystals solubilized by addition of optical grade DMSO (100 μL) over 30 min. Absorbance was measured at 540 nm using a microtitre plate reader. Cell viability was expressed as a percentage of the viability of untreated control cells (mean ± SEM). Each experiment was performed in triplicate, with 6 replicates per experiment.

2.7. Fibroblast attachment assay

Attachment of normal dermal fibroblasts to HA fractions was performed according to (Cook et al., 2000) and (Stephens et al., 2004). First, HA solutions (0.1 mL/well, 2 mg/mL in PBS, 0.2 μm filter-sterilized) were added to wells of a sterile 96-well microtitre plate and incubatedovernightat 4 °C. Control wells were prepared containing BSA solution (0.1 mL/well, 2%, w/v). Non-specific cell binding was blocked byincubation with BSA (2%, w/v in PBS) for 30 min. Cells were then resuspendedin serum-free medium, seeded at 2.5×10^5 cells/mL (0.1 mL/well, 6 replicates) and incubated for 3 h at 37 °C/5% CO_2. Adherent cells were washed (×3) in PBS, fixed in ethanol (70%, v/v, 15 min) and stained with crystal violet solution (0.1 mL/well, 0.1%, w/v, 25 min). Excess dye was removed by washing with H_2O (×3), the bound dye solubilizedusing Triton X-100 solution (0.2%, v/v, 25 μL/well) and the absorbance read at 550 nm. Each experiment was performed in triplicate.

2.8. Statistical analysis

Data were expressed as mean ± the standard error of the mean (SEM). Statistical significance was set at $p < 0.05$ (indicated by *). Evaluation of significance was achieved using a one-way analysis of variance (ANOVA), followed by Bonferroni post-hoc tests that correct for multiple comparisons. All statistical calculations were performed using GraphPad Prism, version 4.0c for Macintosh, 2005.

3. Results and discussion

3.1. Acid hydrolysis of HA

The hydrolysis of HA in dilute HCl was studied at various temperatures by GPC analysis of the reaction mixtures at regular intervals (Fig. 1a and b). To determine if any side reactions occurred, an HA sample degraded in 0.4 M HCl for 16 h at 60 °C (M_w = 70,000 g/mol determined by GPC) was analyzed by FTIR. The spectrum obtained is shown in Fig. 1c. No additional peaks could be seen in the spectrum, compared to the native HA. The HAs used for subsequent experiments and their hydrolysis conditions are detailed in Table 2.

Here, the reaction conditions for HA hydrolysis were optimized using various temperatures and reaction times. At higher temperatures, the molecular weight dropped rapidly while a negligible change was observed at 20 °C. In all cases, polydispersity was high (>1.5), and was highest for HA4 (70,000 g/mol). Polysaccharides, such as HA, usually degrade by random hydrolysis of their glycosidic linkages, yielding a linear relationship between the inverse value of the average molecular weight change ($1/M_w - 1/M_{w,0}$) and time. This was true at all temperatures, with kinetic rate constants of 4.58×10^{-8}, 2.59×10^{-7} and 1.21×10^{-6} at 20, 40 and 60 °C, respectively, derived from the slope of the fitted linear regression curves. Increasing the reaction temperature from 40 to 60 °C accelerated HA hydrolysis nearly 5-fold. Tømmeraas and Melander also observed similar rates of hydrolysis in a recent study (Tommeraas and Melander, 2008).

3.2. Effect of molecular weight on solution properties of HA (diffusion and viscosity)

NMR diffusion measurements are a convenient approach to estimating the conformation of a polymer in solution via the molecular weight scaling dependence of the self-diffusion coefficient. The self-diffusion coefficient may be determined from the slope of an attenuation plot (Eq. (1)), in which the signal amplitude is plotted against the gradient parameter describing the intensity and duration of the field-gradient pulse. Fast diffusion leads to a rapid attenuation of the NMR signal whereas slow diffusion results in a

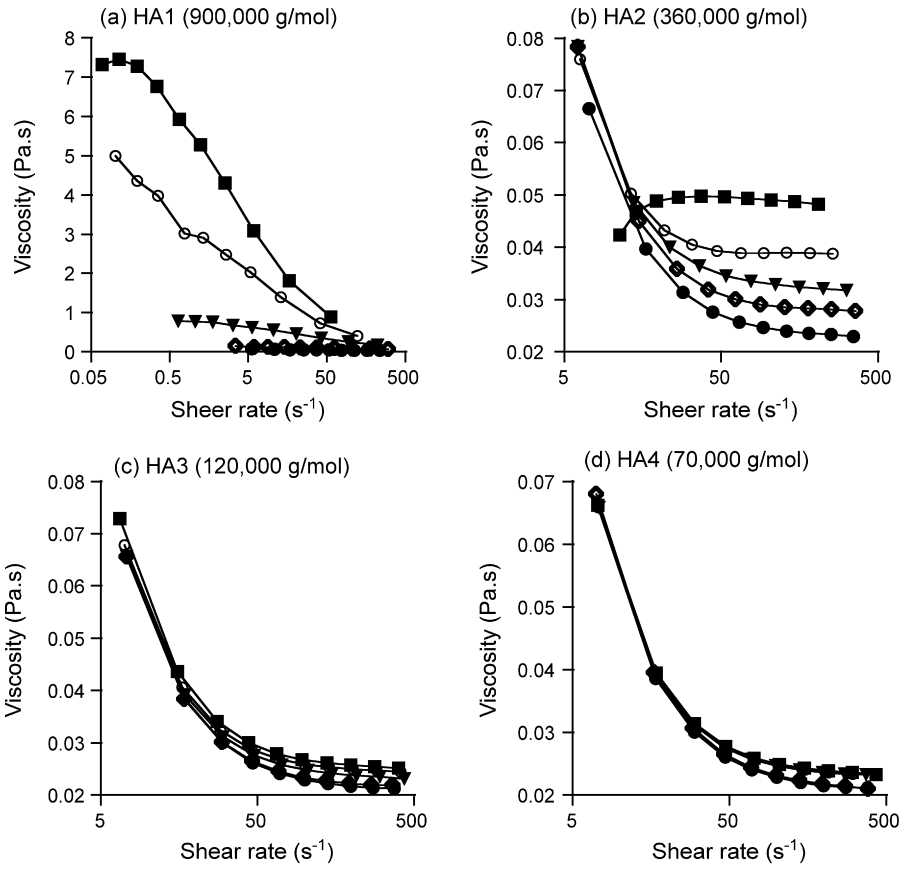

Fig. 3. Viscosity of HA fragments. Panels (a–d) show the viscosity of native HA1 (900,000 g/mol), HA2 (360,000 g/mol), HA3 (120,000 g/mol) and HA4 70,000 g/mol, respectively, at various concentrations, where ■ = 10 mg/mL; ○ = 8 mg/mL; ▼ = 6 mg/mL; ◊ = 4 mg/mL and ● = 2 mg/mL.

far weaker decay in the signal. Exemplar data are given in Fig. 2a, where data pertaining to four polymer samples are presented, at fixed HA concentration (10 mg/mL), a trade-off between sufficient NMR signal and the assumption of a dilute solution. As expected, the self-diffusion coefficient decreases with increasing molecular weight (45,000 > 70,000 > 360,000 > 900,000 g/mol). The linearity of the slopes suggest that the polydispersity of the HA fragments does not significantly perturb the analysis of the data.

Fig. 2b displays the hydrodynamic radii calculated from these self-diffusion coefficients via the Stokes–Einstein equation, plotted in terms of the GPC determined molecular weights. A simple power law relationship exists, $R_h \alpha M_W^{+1}$, indicative of an highly extended, almost rod-like solution conformation, in good agreement with the charged (electrostatic repulsion) character of the polymer backbone.

Further insight into the solution properties was gained by examining the solution viscosities of a series of HA solutions spanning a physiologically relevant concentration and molecular weight range. The strongly shear-thinning character of these solutions is consistent with the polyelectrolyte character of the polymer (McKee et al., 2006), but a number of comparisons may be drawn. In all cases, the viscosity of HA solutions increased with higher HA concentrations (0 < 2 < 4 < 6 < 8 < 10 mg/mL) and chain length (70,000 < 120,000 < 360,000 < 900,000 g/mol) (Fig. 3).

When HA fragments were incubated with HAase for 10 min, viscosity decreased in a concentration-dependent manner (Fig. 4a). Native HA displayed the most significant change in viscosity in the presence of HAase. A linear correlation was seen for higher molecular weight HAs (≥360,000 g/mol) between the logarithm of HAase concentration and HA's viscosity after a 10 min incubation (Fig. 4b).

We investigated the rheological properties of HA at a concentration range of 2–10 mg/mL, since the concentration of HA typically found in human tissues ranges from 0.1 to 5 mg/mL (Kogan et al., 2007). Here, we found that viscosity was chain length- and concentration-dependent. Intra-articular application (viscosupplementation) of high molecular weight HA (1,000,000–7,000,000 g/mol) is commonly used in orthopedic surgery and rheumatology, where its viscoelastic properties mimic those of the synovial fluid (Abate et al., 2010). While these properties may be ideal for viscosupplementation, high viscosity may prevent the efficient conjugation of bioactives. Moreover, highly viscous polymers will not penetrate tissues to deliver their drug payload as easily as less viscous ones. At molecular weights of <360,000 g/mol, very little concentration-dependent change in viscosity was observed in these studies.

In the body, HA degradation is predominantly mediated by HAases (HYAL1 and HYAL2) (Stern and Jedrzejas, 2006), which act by random degradation mechanisms and result in the formation of lower molecular weight fragments of approximately 50 dissacharide units (~20,000 g/mol). During inflammation and/or oxidative stress, HA degradation is increased and is accompanied by reduced viscoelastic properties. Hence, viscoelasticity can be used as a marker of HA degradation. Here, we observed that addition of physiologically relevant concentrations of HAase rapidly reduced HA viscosity in a concentration-dependent manner. While this trend was observed for high molecular weight HA (≥360,000 g/mol), little change was seen with smaller HA chains.

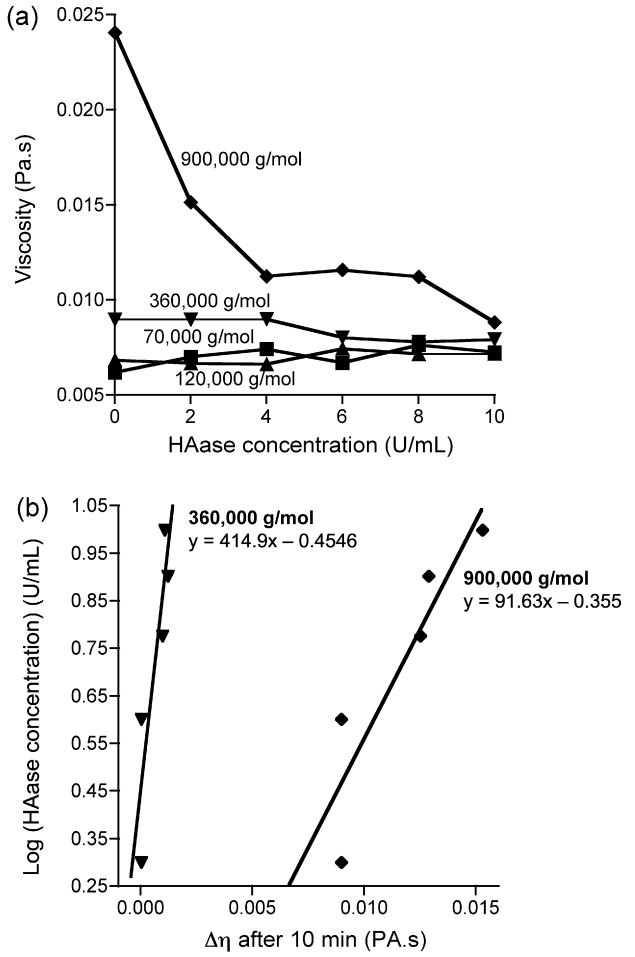

Fig. 4. Viscosity of HA fragments in the presence of HAase. Panel (a) shows viscosity of HA solutions after 10 min incubation with HAase (0–10 U/mL), where ♦ = HA1 (900,000 g/mol); ▼ = HA2 (360,000 g/mol); ▲ = HA3 (120,000 g/mol) and ■ = HA4 (70,000 g/mol). Panel (b) shows the logarithm of HAase concentration plotted against viscosity at 10 min, where ♦ = HA1 (900,000 g/mol) and ▼ = HA2 (360,000 g/mol). $n = 1$.

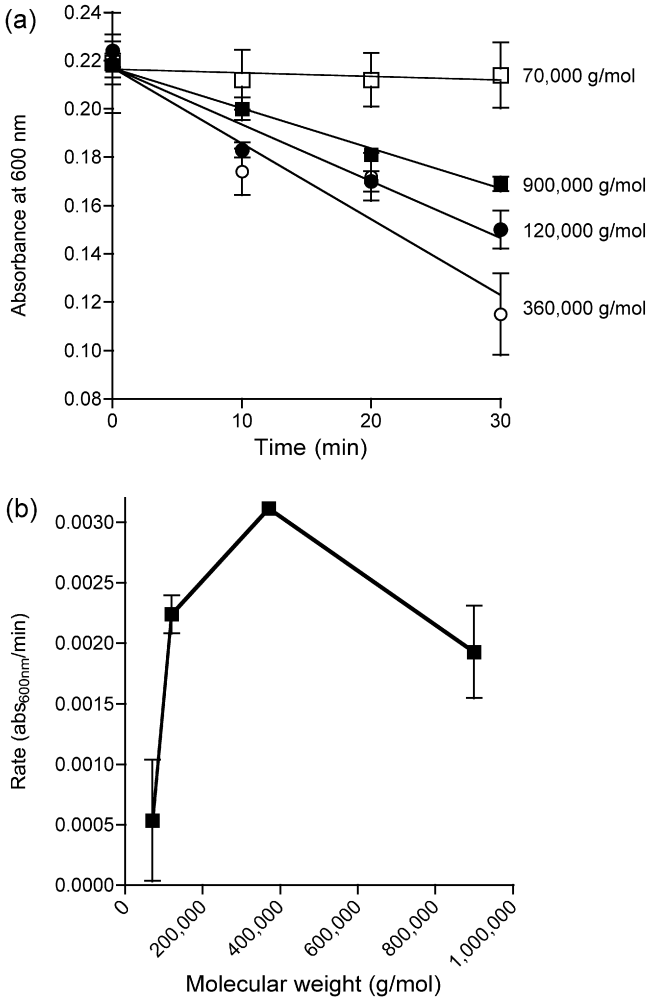

Fig. 5. HAase activity towards HA fragments. Panel (a) shows absorbance changes over time during hydrolysis of HA (160 μg/mL) by HAase (4 U/mL). Panel (b) shows initial hydrolysis rate (determined from kinetic curves shown in panel (a)) plotted against molecular weight of HA fractions.

3.3. Hyaluronidase activity towards HA fragments

HAase-catalyzed degradation of HA was highly variable for different chain lengths (Fig. 5). The slowest rates of hydrolysis were observed for the low molecular weight HA. However, the rate of HAase-mediated degradation increased for larger HA fragments, but decreased once again for the native HA.

Here, initial hydrolysis rate correlated strongly with HA chain length. In accordance with (Deschrevel et al., 2008), we found that shorter chains were too small to form a stable enzyme–substrate complex, while larger chains were hindered, probably through steric hindrance, from forming a complex. This variation in HA degradation rate could be utilized to tailor drug release from HA conjugates, depending on its clinical application, route of administration and dosing schedule. Pathological conditions, such as chronic wounds, inflammation and cancer, typically give rise to elevated concentrations of HAase and/or HA in acidic environments. Therefore, under these conditions, HA degradation rate and subsequent drug release, would be further enhanced.

3.4. HA fragment effects on fibroblast proliferation

The concentration-dependent proliferative activity of native HA and its derivatives on chronic wound and normal dermal fibroblasts is shown in Fig. 6a and b. In all cases, addition of HA, up to 1000 μg/mL, did not significantly affect fibroblast proliferation. However, when normal fibroblasts were incubated with HA1 (900,000 g/mol) at 1000 μg/mL, proliferation was reduced to 62% of untreated cells ($p < 0.001$). Similarly, when chronic wound fibroblasts were incubated with HA4 (70,000 g/mol) at 1000 μg/mL, proliferation was reduced to 73% of untreated cells ($p < 0.001$).

Dermal fibroblasts are pivotal for healing and scarring. Previous literature has demonstrated that the addition of HA can stimulate fibroblast proliferation and collagen production in vitro

Fig. 6. Proliferation of normal and chronic wound fibroblasts (assessed using the MTT assay) in the presence of HA fragments. Panels (a and c) show proliferation of normal fibroblasts after 72 h, in the presence of HA fragments at various concentrations. Panels (b and d) show proliferation of chronic wound fibroblasts after 72 h, in the presence of HA fragments at various concentrations. Where □ = HA1 (900,000 g/mol); ▩ = HA2 (360,000 g/mol); = HA3 (120,000 g/mol) and ▩ = HA4 (70,000 g/mol) for panels (a and b), and where ♦ = HA1 (900,000 g/mol); × = HA2 (360,000 g/mol); ○ = HA3 (120,000 g/mol) and ■ = HA4 (70,000 g/mol) for panels (c and d). Data represent mean ± SEM, $n = 18$. Where error bars are invisible they are within size of data points. Asterisks (**) indicate significance $p < 0.001$ compared to control.

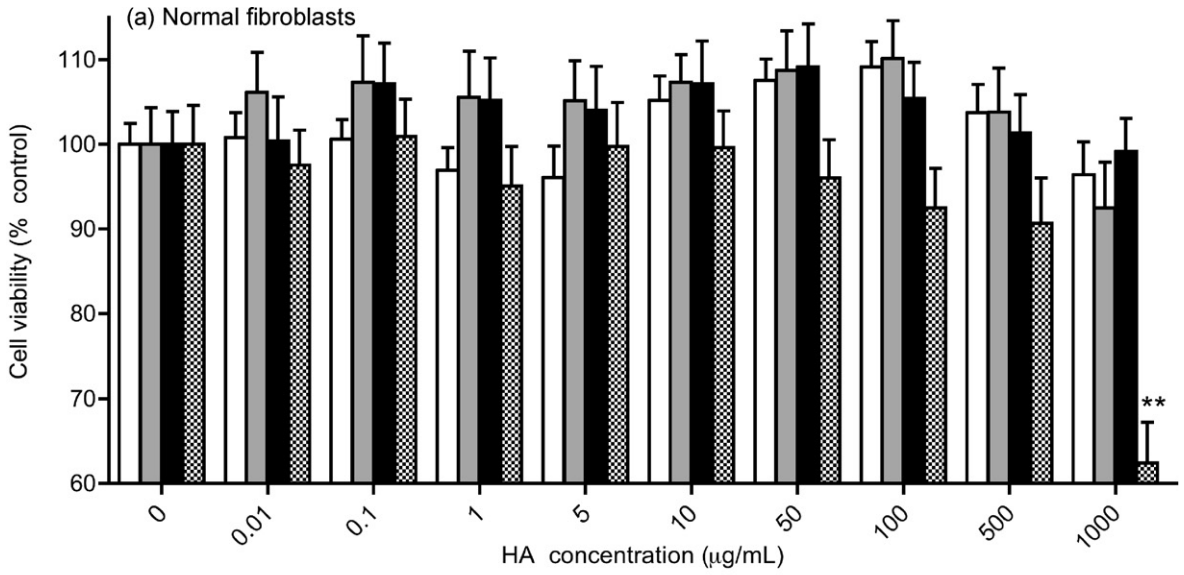
(a) Normal fibroblasts
Cell viability (% control)
110
100
90
80
70
60
**
0
0.01
0.1
1
5
10
50
100
500
1000
HA concentration (μg/mL)

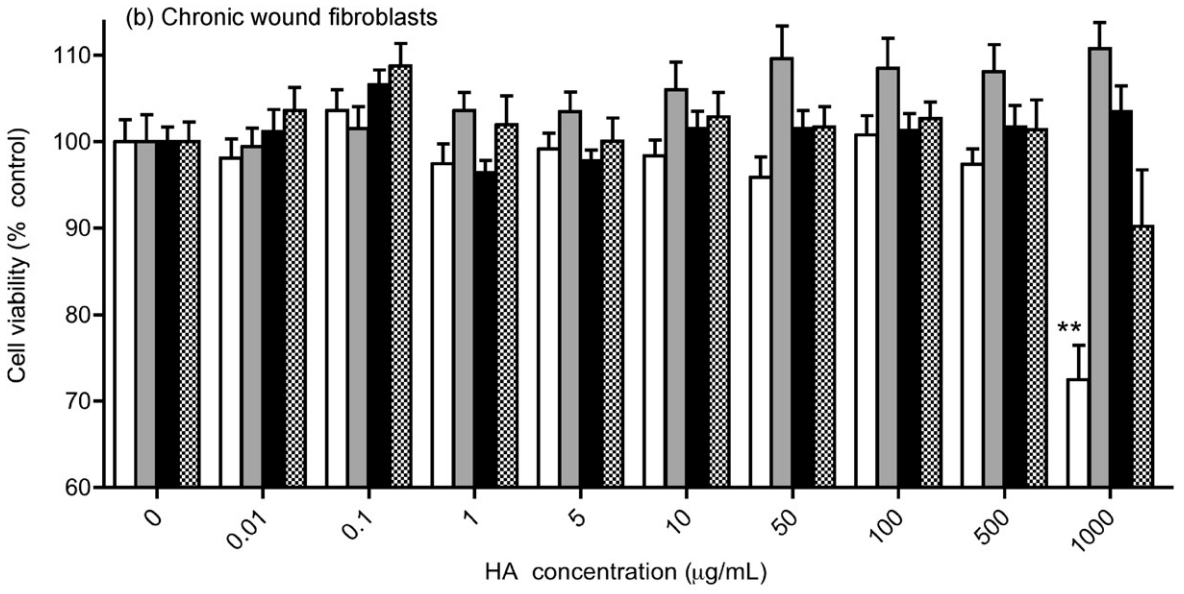
(b) Chronic wound fibroblasts
Cell viability (% control)
110
100
90
80
70
60
**
0
0.01
0.1
1
5
10
50
100
500
1000
HA concentration (μg/mL)

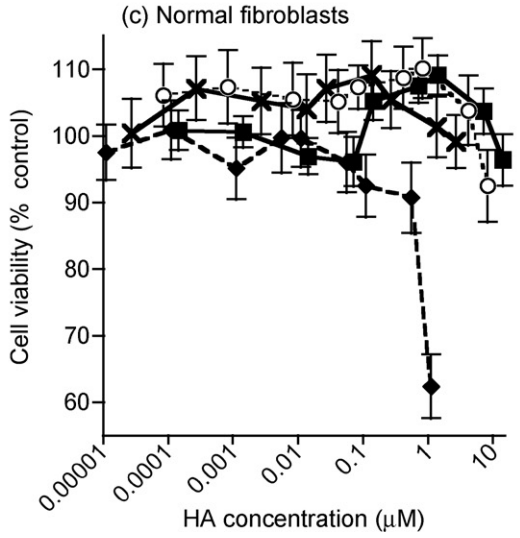
(c) Normal fibroblasts
Cell viability (% control)
110
100
90
80
70
60
0.00001
0.0001
0.001
0.01
0.1
1
10
HA concentration (μM)

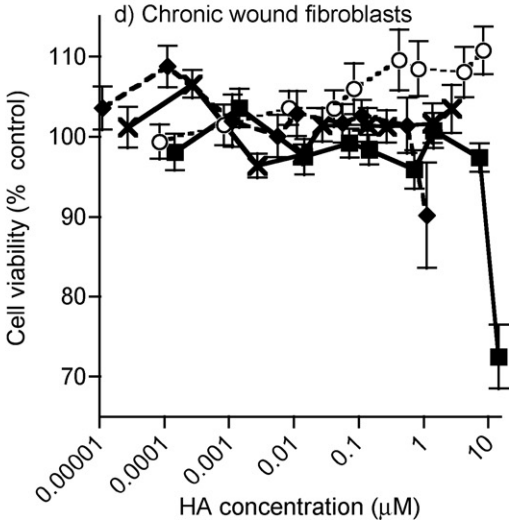
d) Chronic wound fibroblasts
Cell viability (% control)
110
100
90
80
70
0.00001
0.0001
0.001
0.01
0.1
1
10
HA concentration (μM)

(Greco et al., 1998; Huang et al., 2009). Here, we have shown that the addition of HA to normal and chronic wound-derived fibroblasts generally did not significantly affect their proliferation. When Greco et al. (1998) entrapped HA (1,100,000 g/mol, 150 μg/mL) in fibroblast-populated collagen lattices, they reported stimulation in cell division. However, when the same cells were grown in a monolayer, cell proliferation in the presence of HA was the same as untreated cells.

Interestingly, our results showed that while high concentrations of 900,000 g/mol HA significantly inhibited proliferation of normal fibroblasts, equivalent concentrations of 70,000 g/mol HA significantly reduced the proliferation of chronic wound-derived cells. Consequently, polymer conjugates should be carefully designed to have a relatively high protein loading to facilitate delivery of therapeutic quantities of bioactive agent, while maintaining the concentration of HA below the anti-proliferative threshold. It has previously been shown that HA's chain length, as well as its concentration, determines its physiological function, such that high concentrations of HMW HA inhibited cell growth in 3T3 synovial cells (Goldberg and Toole, 1987). The effect seen in chronic wound fibroblasts does not follow this trend, which reflects the biological alterations in these cells within a chronically inflamed wound bed, in terms of their phenotype, reduced proliferative life-span and the early onset of cellular senescence (Wall et al., 2008). It is likely that this is, in part, due to the differential HA synthesis and/or expression of HA cell-surface receptors on chronic wound fibroblasts, given that Wall et al. (2008) showed that there is >2-fold greater induction of hyaluronan synthase 1 (HAS1) in chronic wound fibroblasts, compared to normal dermal fibroblasts. Furthermore, it has been reported that HAase activity in pressure ulcers was significantly elevated, compared with acute wounds (10.4 ± 0.5 and 5.17 ± 0.17 mU/ng DNA, respectively) (Dechert et al., 2006). The authors suggest that the increased enzymatic degradation of HA leads to inflammation during wound repair. Although the chronic wound fibroblasts used in our studies may have higher HAase activity than the normal fibroblasts, it is highly likely that, during the 72 h incubation, all HA fragments were fully degraded in both the chronic wound and normal fibroblasts. This could explain why HA fragment size generally did not significantly affect fibroblast proliferation in our studies.

When HA concentration was considered in molar concentration, the effect of the number of HA chains on proliferation could be seen. Here, 900,000 g/mol HA inhibited fibroblast proliferation more at lower molar concentrations, than the shorter HA chains with both normal and chronic wound fibroblasts (Fig. 6c and d). There are three well-characterized cell surface receptors for HA: CD44, hyaluronan-mediated motility receptor (RHAMM) and toll-like receptor (TLR) -2 and -4 (Evanko et al., 2007). One-to-one binding of HA to these receptors triggers a signaling cascade, which regulates cell–cell interactions, cell adhesion, angiogenesis and migration. This observation supports the use of low concentration and low molecular weight HA when designing a polymer conjugate for enhanced tissue repair.

3.5. Fibroblast attachment

Native HA inhibited normal dermal fibroblast adhesion to the same extent as BSA after 3 h ($p > 0.05$) (Fig. 7). Smaller chains of HA promoted cell attachment in a size-dependant manner (70,000 > 120,000 > 360,000 > 900,000 g/mol). For 70,000, 120,000 and 360,000 g/mol HA fragments, cell adhesion was significantly greater than that of BSA-coated control wells ($p < 0.001$, $p < 0.001$, $p < 0.05$, respectively), while native not statistically different to BSA-coated wells ($p > 0.05$).

HA-coated surfaces promoted fibroblast attachment in a molecular weight-dependent manner. Native HA-coated surfaces

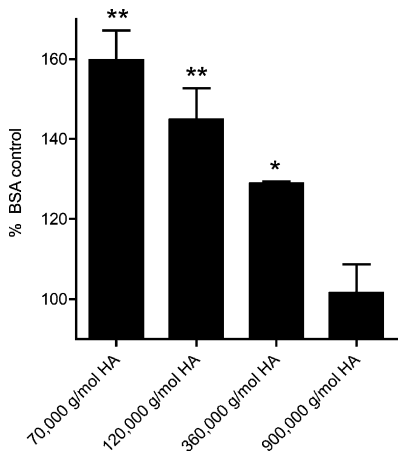

Fig. 7. Effect of HA chain length on the attachment of normal dermal fibroblasts to HA-coated surfaces. Data represent mean ± SEM, n = 6. Where error bars are invisible they are within size of data points. Asterisk (*) indicates significance $p < 0.05$ compared to control and ** indicates significance $p < 0.001$ compared to control.

appeared less adhesive than lower molecular weight fragments. Conversely, Huang et al. (2009) demonstrated that supplementation of fibroblast culture medium with HA prevented cellular attachment in a dose-dependent manner. We propose that the increased attachment seen in our studies is due to the different methods used for coating the plates with HA. In a normal wound, fibroblasts are recruited to the wound site by 48 h following injury and migrate though a provisional matrix, largely composed of fibronectin and HA; biopolymers which create a highly hydrated matrix and facilitate cell migration and adhesion. We have previously employed the inert carrier, dextrin, in our growth factor polymer conjugate systems for wound healing (Hardwicke et al., 2008, 2010, 2011). A significant potential advantage of HA-based polymer therapies in this respect is the ability of the carrier to independently potentiate wound healing responses at the site of disease, while effecting cellular delivery of the drug to the wound.

4. Conclusions

As novel targets for polymer therapeutics are identified, there is an increasing need for careful selection of polymeric carriers. Here, it was shown that the physical and biological properties of HA and its fragments are molecular weight-dependent. Acid hydrolysis is an effective means of tailoring the size of native HA, without any detectable side reactions. The differential effects of HA and its fragments is apparent and may play a crucial role in the tissue repair process. Smaller HA fragments promote cell adhesion, migration and proliferation, but are readily degraded by HAase. This study confirms the potential of low molecular weight fractions of HA for protein and peptide delivery for wound repair purposes and precedes further investigations of such HA conjugates.

Acknowledgements

We thank Professor Ruth Duncan for reviewing the manuscript and engaging in useful discussions. We would like to acknowledge support from EPSRC Platform grant no. EP/C 013220/1.

References

Abate, M., Pulcini, D., Di Iorio, A., Schiavone, C., 2010. Viscosupplementation with intra-articular hyaluronic acid for treatment of osteoarthritis in the elderly. Curr. Pharm. Des. 16, 631–640.

Bhang, S.H., Won, N., Lee, T.J., Jin, H., Nam, J., Park, J., Chung, H., Park, H.S., Sung, Y.E., Hahn, S.K., Kim, B.S., Kim, S., 2009. Hyaluronic acid-quantum dot conjugates for *in vivo* lymphatic vessel imaging. ACS Nano 3, 1389–1398.

Cai, S., Xie, Y., Bagby, T.R., Cohen, M.S., Forrest, M.L., 2008. Intralymphatic chemotherapy using a hyaluronan–cisplatin conjugate. J. Surg. Res. 147, 247–252.
Chen, W.Y., Abatangelo, G., 1999. Functions of hyaluronan in wound repair. Wound Repair Regen. 7, 79–89.
Cook, H., Davies, K.J., Harding, K.G., Thomas, D.W., 2000. Defective extracellular matrix reorganization by chronic wound fibroblasts is associated with alterations in TIMP-1, TIMP-2, and MMP-2 activity. J. Invest. Dermatol. 115, 225–233.
Cui, X., Xu, H., Zhou, S., Zhao, T., Liu, A., Guo, X., Tang, W., Wang, F., 2009. Evaluation of angiogenic activities of hyaluronan oligosaccharides of defined minimum size. Life Sci. 85, 573–577.
Davies, J.A., Griffiths, P.C., 2003. A phenomenological approach to separating the effects of obstruction and binding for the diffusion of small molecules in polymer solutions. Macromolecules 36, 950–952.
Dechert, T.A., Ducale, A.E., Ward, S.I., Yager, D.R., 2006. Hyaluronan in human acute and chronic dermal wounds. Wound Repair Regen. 14, 252–258.
Deschrevel, B., Tranchepain, F., Vincent, J.C., 2008. Chain-length dependence of the kinetics of the hyaluronan hydrolysis catalyzed by bovine testicular hyaluronidase. Matrix Biol. 27, 475–486.
Dorfman, A., Ott, M.L., 1948. A turbidimetric method for the assay of hyaluronidase. J. Biol. Chem. 172, 367–375.
Duncan, R., 2003. The dawning era of polymer therapeutics. Nature Rev. Drug Discov. 2, 347–360.
Duncan, R., Gilbert, H.R.P., Carbajo, R.J., Vicent, M.J., 2008. Polymer masked-unmasked protein therapy (PUMPT) 1. Bioresponsive dextrin–trypsin and -MSH conjugates designed for α-amylase activation. Biomacromolecules 9, 1146–1154.
Evanko, S.P., Tammi, M.I., Tammi, R.H., Wight, T.N., 2007. Hyaluronan-dependent pericellular matrix. Adv. Drug Deliv. Rev. 59, 1351–1365.
Ferguson, E.L., Alshame, A.M., Thomas, D.W., 2010. Evaluation of hyaluronic acid–protein conjugates for polymer masked-unmasked protein therapy. Int. J. Pharm. 402, 95–102.
Gaspar, R., Duncan, R., 2009. Polymeric carriers: preclinical safety and the regulatory implications for design and development of polymer therapeutics. Adv. Drug Deliv. Rev. 61, 1220–1231.
Gilbert, H.R.P., 2007. Bioresponsive polymer–protein conjugates as a unimolecular drug delivery system. PhD Thesis, Cardiff University, Cardiff, UK.
Gilbert, H.R.P., Duncan, R., 2006. Polymer–protein conjugates for triggered activation: hyaluronic acid–trypsin as a model. In: Proc. Ann. Meet. Control. Release Soc., Vienna, Austria, vol. 33, p. 661.
Goldberg, R.L., Toole, B.P., 1987. Hyaluronate inhibition of cell proliferation. Arthritis Rheum. 30, 769–778.
Greco, R.M., Iocono, J.A., Ehrlich, H.P., 1998. Hyaluronic acid stimulates human fibroblast proliferation within a collagen matrix. J. Cell Physiol. 177, 465–473.
Hardwicke, J., Ferguson, E.L., Moseley, R., Stephens, P., Thomas, D., Duncan, R., 2008. Dextrin–rhEGF conjugates as bioresponsive nanomedicines for wound repair. J. Control. Release 130, 275–283.
Hardwicke, J., Moseley, R., Stephens, P., Harding, K., Duncan, R., Thomas, D.W., 2010. Bioresponsive dextrin–rhEGF conjugates: *in vitro* evaluation in models relevant to its proposed use as a treatment for chronic wounds. Mol. Pharm. 7, 699–707.
Hardwicke, J.T., Hart, J., Bell, A., Duncan, R., Thomas, D.W., Moseley, R., 2011. The effect of dextrin–rhEGF on the healing of full-thickness, excisional wounds in the (db/db) diabetic mouse. J. Control. Release 152, 411–417.
Herrick, S.E., Sloan, P., McGurk, M., Freak, L., McCollum, C.N., Ferguson, M.W., 1992. Sequential changes in histologic pattern and extracellular matrix deposition during the healing of chronic venous ulcers. Am. J. Pathol. 141, 1085–1095.
Homma, A., Sato, H., Okamachi, A., Emura, T., Ishizawa, T., Kato, T., Matsuura, T., Sato, S., Tamura, T., Higuchi, Y., Watanabe, T., Kitamura, H., Asanuma, K., Yamazaki, T., Ikemi, M., Kitagawa, H., Morikawa, T., Ikeya, H., Maeda, K., Takahashi, K., Nohmi, K., Izutani, N., Kanda, M., Suzuki, R., 2009. Novel hyaluronic acid–methotrexate conjugates for osteoarthritis treatment. Bioorg. Med. Chem. 17, 4647–4656.
Huang, L., Gu, H., Burd, A., 2009. A reappraisal of the biological effects of hyaluronan on human dermal fibroblast. J. Biomed. Mater. Res. A 90, 1177–1185.
Itano, N., 2008. Simple primary structure, complex turnover regulation and multiple roles of hyaluronan. J. Biochem. 144, 131–137.
Ito, T., Fraser, I.P., Yeo, Y., Highley, C.B., Bellas, E., Kohane, D.S., 2007. Anti-inflammatory function of an *in situ* cross-linkable conjugate hydrogel of hyaluronic acid and dexamethasone. Biomaterials 28, 1778–1786.
Kogan, G., Soltes, L., Stern, R., Gemeiner, P., 2007. Hyaluronic acid: a natural biopolymer with a broad range of biomedical and industrial applications. Biotechnol. Lett. 29, 17–25.
Linker, A., Mayer, K., 1954. Production of unsaturated uronides by bacterial hyaluronidases. Nature 174, 1192–1193.
McKee, M.G., Hunley, M.T., Layman, J.M., Long, T.E., 2006. Solution rheological behavior and electrospinning of cationic polyelectrolytes. Macromolecules 39, 575–583.
Mosmann, T., 1983. Rapid colorimetric assay for cellular growth and survival: application to proliferation and cytotoxicity assays. J. Immunol. Methods 65, 55–63.
Oh, E.J., Kim, J.W., Kong, J.H., Ryu, S.H., Hahn, S.K., 2008. Signal transduction of hyaluronic acid–peptide conjugate for formyl peptide receptor like 1 receptor. Bioconjug. Chem. 19, 2401–2408.
Oh, E.J., Park, K., Kim, K.S., Kim, J., Yang, J.A., Kong, J.H., Lee, M.Y., Hoffman, A.S., Hahn, S.K., 2010. Target specific and long-acting delivery of protein, peptide, and nucleotide therapeutics using hyaluronic acid derivatives. J. Control. Release 141, 2–12.
Price, R.D., Berry, M.G., Navsaria, H.A., 2007. Hyaluronic acid: the scientific and clinical evidence. J. Plast. Reconstr. Aesthetic Surg. 60, 1110–1119.
Schanté, C.E., Zuber, G., Herlin, C., Vandamme, T.F., 2011. Chemical modifications of hyaluronic acid for the synthesis of derivatives for a broad range of biomedical applications. Carbohydr. Polym. 85, 469–489.
Stephens, P., Grenard, P., Aeschlimann, P., Langley, M., Blain, E., Errington, R., Kipling, D., Thomas, D., Aeschlimann, D., 2004. Crosslinking and G-protein functions of transglutaminase 2 contribute differentially to fibroblast wound healing responses. J. Cell Sci. 117, 3389–3403.
Stern, R., Jedrzejas, M.J., 2006. Hyaluronidases: their genomics, structures, and mechanisms of action. Chem. Rev. 106, 818–839.
Stern, R., Maibach, H.I., 2008. Hyaluronan in skin: aspects of aging and its pharmacologic modulation. Clin. Dermatol. 26, 106–122.
Tommeraas, K., Melander, C., 2008. Kinetics of hyaluronan hydrolysis in acidic solution at various pH values. Biomacromolecules 9, 1535–1540.
Varghese, O.P., Sun, W., Hilborn, J., Ossipov, D.A., 2009. In situ cross-linkable high molecular weight hyaluronan–bisphosphonate conjugate for localized delivery and cell-specific targeting: a hydrogel linked prodrug approach. J. Am. Chem. Soc. 131, 8781–8783.
Wall, I.B., Moseley, R., Baird, D.M., Kipling, D., Giles, P., Laffafian, I., Price, P.E., Thomas, D.W., Stephens, P., 2008. Fibroblast dysfunction is a key factor in the non-healing of chronic venous leg ulcers. J. Invest. Dermatol. 128, 2526–2540.
Wang, C.T., Lin, J., Chang, C.J., Lin, Y.T., Hou, S.M., 2004. Therapeutic effects of hyaluronic acid on osteoarthritis of the knee. A meta-analysis of randomized controlled trials. J. Bone Joint Surg. 86, 538–545.
West, D.C., Kumar, S., 1989. The effect of hyaluronate and its oligosaccharides on endothelial cell proliferation and monolayer integrity. Exp. Cell Res. 183, 179–196.